Atmos. Chem. Phys. Discuss., https://doi.org/10.5194/acp-2018-855
Manuscript under review for journal Atmos. Chem. Phys.
Discussion started: 11 September 2018

Atmospheric Chemistry and Physics Discussions

Evidence for a major missing source in the global chloromethane budget from stable carbon isotopes

Enno Bahlmann[1,2], Frank Keppler[3,4,5], Julian Wittmer[6,7], Markus Greule[3,4], Heinz Friedrich Schöler[3], Richard Seifert[1], Cornelius Zetzsch[5,6]

[1]Institute of Geology, University Hamburg, Bundesstrasse 55, 20146 Hamburg, Germany
[2]Leibniz Centre for Tropical Marine Research, Fahrenheitstraße 6, 28359 Bremen
[3]Institute of Earth Sciences, Heidelberg University, Im Neuenheimer Feld 234-236, 69120 Heidelberg, Germany
[4]Heidelberg Center for the Environment (HCE), Heidelberg University, 69120 Heidelberg, Germany
[5]Max-Planck-Institute for Chemistry, Hahn-Meitner-Weg 1, 55128 Mainz, Germany
[6]Atmospheric Chemistry Research Unit, BayCEER, University of Bayreuth, Dr Hans-Frisch Strasse 1–3, 95448 Bayreuth, Germany
[7]Agilent Technologies Sales & Services GmbH & Co. KG, Hewlett-Packard-Str. 8, 76337 Waldbronn, Germany

Correspondence to: Enno Bahlmann enno.bahlmann@zmt-leibniz.de

Abstract. Chloromethane (CH_3Cl) is the most important natural input of reactive chlorine to the stratosphere, contributing about 16% to stratospheric ozone depletion. Due to the phase out of anthropogenic emissions of chlorofluorocarbons, CH_3Cl will largely control future levels of stratospheric chlorine.

The tropical rainforest is commonly assumed to be the strongest single CH_3Cl source, contributing over half of the global annual emissions of about 4000 to 5000 Gg (1 Gg = 10^9 g). This source shows a characteristic carbon isotope fingerprint, making isotopic investigations a promising tool for improving its atmospheric budget. Applying carbon isotopes to better constrain the atmospheric budget of CH_3Cl requires sound information on the kinetic isotope effects for the main sink processes e.g. the reaction with OH and Cl in the troposphere. We conducted photochemical CH_3Cl degradation experiments in a 3500L smog chamber to determine the carbon isotope fractionation (ε) for the reaction of CH_3Cl with OH and Cl. For the reaction of CH_3Cl with OH, we determined a ε of (-11.2±0.8) ‰ (n=3) and for the reaction with Cl we found a ε of (-10.2±0.5) ‰ (n=1) being five to six times smaller than previously reported. Our smaller isotope effects are strongly supported by the lack of any significant seasonal covariation in previously reported tropospheric $\delta^{13}C(CH_3Cl)$ values with the OH driven seasonal cycle in tropospheric mixing ratios.

Applying these new fractionation factors to the global CH_3Cl budget using a simple two hemispheric box model, we derive a tropical rainforest CH_3Cl source of (670±200) Gg a^{-1}, which is considerably smaller than previous estimates. A revision of previous bottom up estimates, using above ground biomass instead of rainforest area, strongly supports this lower estimate. Finally, our results suggest a large unknown tropical CH_3Cl source of (1230±200) Gg a^{-1}.

1 1 Introduction

In the mid-90s, the recognition that the known CH_3Cl sources, mainly biomass burning and marine emissions, are insufficient to balance the known atmospheric sinks (Butler, 2000) motivated intense research on potential terrestrial sources. Today, it is common thinking that large emissions from tropical rainforests (Monzka et al., 2010; Xiao et al, 2010; Carpenter et al., 2014) can close this gap. Several model studies revealed a strong tropical CH_3Cl source in the range of 2000 Gg a^{-1} (Xiao et al. 2010, Yoshida et al., 2004, Lee Taylor et al. 1998). Particular support for a strong tropical rainforest source arose from observations of elevated CH_3Cl concentrations in the vicinity of tropical

Atmos. Chem. Phys. Discuss., https://doi.org/10.5194/acp-2018-855
Manuscript under review for journal Atmos. Chem. Phys.
Discussion started: 11 September 2018

rainforests (Yokouchi et al., 2000), greenhouse experiments (Yokouchi et al., 2002), several field measurements in tropical rainforests (Saito et al. 2008; Gebhardt et al. 2008; Blei et al., 2010; Saito et al., 2013 and from carbon stable isotope mass balances (Keppler et al. 2005; Saito & Yokouchi, 2008). The majority of CH_3Cl in tropical rain forests ((2000±600) Gg a^{-1}) is thought to originate from higher plants (Monzka et al., 2010; Xiao et al, 2010; Yokouchi et al. 2000; Saito & Yokouchi, 2008). A minor fraction of about 150 Gg a^{-1} may be emitted from wood rotting fungi (Monzka et al., 2010; Xiao et al, 2010; Carpenter et al., 2014). Further emissions from senescent leaf litter (Keppler et al. 2005) may substantially contribute to this source, but this has not yet been confirmed in field studies (Blei et al. 2010). On a global scale, biomass burning ((400 to 1100) Gg a^{-1}) and surface ocean net emissions (140 to 640 Gg a^{-1}) are further important sources (Monzka et al., 2010; Xiao et al, 2010; Carpenter et al., 2014). Chloromethane from higher plants has an average stable isotope signature ($^{13}C/^{12}C$ ratio, $\delta^{13}C$ value) of (-83±15) ‰ (Saito et al., 2008; Saito & Yokouchi, 2008). Compared to the other known sources with $\delta^{13}C$ values in the range from -36 ‰ to -62 ‰ (Keppler et al. 2005; Saito & Yokouchi, 2008), the tropical rainforest source is exceptionally depleted in ^{13}C making stable isotope approaches particular useful to better constrain CH_3Cl flux estimates.

The isotopic composition of tropospheric CH_3Cl links the isotopic source signatures to the kinetic isotope effects (KIEs) of the sinks. The primary CH_3Cl sink is its oxidation in the troposphere by OH and Cl, accounting for about 80% of total losses (Monzka et al., 2010; Xiao et al, 2010; Carpenter et al., 2014). Further sinks comprise soil uptake and loss to the stratosphere (Monzka et al., 2010; Xiao et al, 2010; Carpenter et al., 2014). An accurate determination of the KIEs of the bulk tropospheric sink (OH + Cl) is crucial for constraining the tropical rainforest source from an isotopic perspective. A previous study (Gola et al. 2005) revealed large KIEs of (-59±8) ‰ and (-70±10) ‰ for the reaction of CH_3Cl with OH and Cl, respectively, which supported the hypothesis of large emissions from tropical rainforests (Keppler et al., 2005; Saito & Yokouchi, 2008). In particular, the KIE for the reaction with OH is much larger in comparison to previously reported KIEs for the reaction of OH with methane (Saueressig et al., 2001) and other hydrocarbons (Rudolph et al., 2000; Anderson et al., 2004). We thus performed photochemical degradation experiments of CH_3Cl in a 3500 L Teflon smog chamber using established radical generation schemes (see method section for details) to reassess the KIEs for the reaction of CH_3Cl with OH and Cl. For validation purposes, we further determined the known KIEs for the same reactions of methane.

In the next step, we used the seasonal variations in the mixing ratios (Prinn et al., 2000) and isotopic composition (Thompson et al., 2002; Redeker et al., 2007) of tropospheric CH_3Cl to further assess the reliability of the obtained KIEs. This was done with a simple two-box model, dividing the atmosphere into a northern and a southern hemisphere and using a simplified emission scheme. The same model was then used to constrain the tropical rainforest source from an isotopic perspective. We finally improved previous bottom up estimates of the tropical rainforest source using carbon density maps of the tropical rainforest instead of coverage area.

2 The kinetic isotope effect (ε) for the reaction of CH_3Cl with OH and Cl

2.1 Materials and methods

2.1.1 Smog chamber

The smog chamber set up and the experimental conditions are the same as recently described in Keppler et al. (2018). The samples for the carbon isotope analysis were taken from the same experiments described therein. Briefly, the

isotope fractionation experiments were performed in a (3500±100) L Teflon smog-chamber. The chamber was continuously flushed with purified, hydrocarbon-free zero air (zero-air-generator, cmc instruments, <1 nmol mol^{-1} of O_3, <500 pmol mol^{-1} NO_X, <100 nmol mol^{-1} of CH_4) at a rate of 0.6 - 4 L min^{-1} to maintain a slight overpressure of 0.5-1 Pa logged with a differential pressure sensor (Kalinsky Elektronik DS1). A Teflon fan inside the chamber ensured constant mixing throughout the experiments. NO and NO_X were monitored on a routine basis with an EcoPhysics, CLD 88p chemiluminiscence analyzer coupled with an EcoPhysics photolytic converter, PLC 860. Ozone was monitored by a chemiluminescence analyzer (UPK 8001). Initial CH_3Cl mixing ratios were between 5 µmol mol^{-1} and 14 µmol mol^{-1}. Perfluorohexane (PFH) was used as an internal standard with initial mixing ratios of (25±3) µmol mol^{-1} to correct the resulting concentrations for dilution. The mixing ratios of CH_3Cl and perfluorohexane were monitored by GC-MS (Agilent Technologies, Palo Alto, CA) with a time resolution of 15 minutes throughout the experiments. The stability of the instrument was regularly checked using a gaseous standard (5 ml of 100 µmol mol^{-1} CH_3Cl in N_2). Mixing ratios of methane and CO_2, used as internal standard in the methane degradation experiments, were measured with a Picarro G221i cavity ring down spectrometer. Prior to the experiments, the instrument was calibrated with pressurized ambient air from a tank obtained from the Max-Planck-Institute for Biogeochemistry in Jena/Germany (CO_2 mixing ratio of (394.6±0.5) µmol mol^{-1}, methane mixing of (1.752±0.002) µmol mol-1). OH radicals were generated via the photolysis of ozone (about 2 µmol mol^{-1} for CH_3Cl and about 10 µmol mol^{-1} for CH_4) at 253.7 nm in the presence of water vapor (Relative humidity = 70%). This is a well-established efficient method for OH radical generation (Cantrell et al. 1990, DeMore 1992). In the CH_3Cl + OH experiments initially 2000 µmol mol^{-1} of H_2 was added for scavenging chlorine radicals originating from the photolysis or oxidation of formyl chloride (HCOCl) occurring as an intermediate in the reaction cascade (Gola et al., 2005). To obtain an efficient OH formation, Philips TUV lamps (1x55 W for CH_3Cl, 4x55W for CH_4) were welded in Teflon film and mounted inside the smog chamber. Atomic chlorine (Cl) was generated via photolysis of molecular chlorine (Cl_2) at a relative humidity of less than 1% by a solar simulator with an actinic flux comparable to the sun in mid-summer in Germany.. A more detailed description of the experimental setup has recently been published elsewhere (Wittmer et al., 2015; Keppler et al., 2018).

2.1.2 Sampling and carbon isotope determination

From each experiment 10 to 15 canister samples (2 L stainless steel, evacuated <1.3x10^{-3} Pa and baked out) and 10 to 15 adsorption tube samples were taken at regular time intervals for subsequent analysis of carbon isotope ratios. The adsorption tube samples and one set of canister samples from the CH_3Cl degradation experiments were analyzed by 2D-GC-IRMS/MS at the University of Hamburg using the method of Bahlmann et al. (2011). This method has been shown to be free of interferences from other compounds. The precision and reproducibility of the $\delta^{13}C$ measurements based on standards were ± 0.6‰ (n = 18) on the 1σ level. In order to assure compliance with VPDB scale, a single component standard of CH_3Cl (100 µmol mol^{-1} in nitrogen, Linde Germany) was analyzed via the 2D-GC-IRMS. The results were compared to those after offline combustion and analysis via a dual inlet (DI) against a certified CO_2 reference standard (Air Liquide, Germany, -26.8± 0.2‰ and a solid standard (Nist NBS 18, RM 8543). The results from the DI (n=6) were (-37.19 ±0.08) ‰ for CH_3Cl. The respective $\delta^{13}C$ values from the GC-GC/IRMS, measured against the machine working gas (Air Liquide, Germany, (-26.8± 0.2) ‰) were (-36.06±0.21) ‰ resulting in an offset (DI – 2D-GC-IRMS) of -1.13‰ for CH_3Cl. All results were corrected for this offset.

Atmos. Chem. Phys. Discuss., https://doi.org/10.5194/acp-2018-855
Manuscript under review for journal Atmos. Chem. Phys.
Discussion started: 11 September 2018

Atmospheric Chemistry and Physics Discussions

The canister samples were analyzed at the University of Heidelberg using a cryogenic pre-concentration system coupled to a GC-C-IRMS system, developed for δ^2H measurements of CH_3Cl (Greule et al. 2012). Notwithstanding, a combustion reactor filled with copper (II) oxide at 850°C was used to analyze $\delta^{13}C$ The precision and reproducibility of these $\delta^{13}C$ measurements based on a chloromethane working standard were ± 0.47 ‰ (n = 47) on the 1σ level. The $\delta^{13}C$ values measured in both laboratories generally agreed within ± 1.3 ‰ on the 1σ level. Methane carbon isotope ratios were only analyzed at the University of Heidelberg.

2.1.3 Calculation of ε

The carbon isotope ratios are reported in the δ-notation relative to the VPDB scale (Vienna Pee Dee Belemnite) and the isotope fractionation (ε) is reported in [‰]. We applied an orthogonal regression model (Danzer et al. 1995) to derive the KIE for each experiment from the slope of the Rayleigh plot:

$$(\alpha - 1) * \ln(f_t) = ln\left(\frac{\delta^{13}C_t+1000}{\delta^{13}C_0+1000}\right) \quad (1)$$

And

$$\varepsilon = (\alpha - 1) \quad (2)$$

with ε being the enrichment factor, α being the isotopic fractionation factor, f_t being the residual fraction at time t, $\delta^{13}C_0$ being the initial carbon isotope ratio of the substrate [‰], $\delta^{13}C_t$ being the carbon isotope ratio of the substrate [‰] at time t and KIE being the kinetic isotope effect [‰]. To account for the dilution from the air flow through the chamber, the residual fraction (f_t) has been calculated from the mixing ratios of CH_3Cl and the inert tracer PFH as follows:

$$f_t = \frac{[CH_3Cl_t]*[PFH_0]}{[CH_3Cl_0]*[PFH_t]} \quad (3)$$

Here [CH_3Cl] and [PFH] denote the respective concentrations and the indices t and 0 refer to time t and zero respectively. The uncertainty for f_t ranged from 1.4 to 1.8% on the 1σ level.

2.2 Results of the CH_3Cl degradation experiments

In total we performed six degradation experiments and two control experiments within this study. To perform the degradation experiments within a day, the experimental conditions were modified as indicated in table 1. For the OH experiments in the presence of methane the light intensity was increased from 55W to 220W and the steady state ozone mixing ratios were increased from about 620 nmol mol^{-1} to about 3570 nmol mol^{-1}. Under these experimental conditions typically 70 to 80% of the initial CH_3Cl and methane were degraded within 6 to 10h. For a more detailed discussion of the experimental conditions with respect to the OH yields and degradation rates, the reader is referred to Keppler et al. (2018) reporting on the hydrogen isotope effects from these experiments.

Prior each degradation experiment, we monitored the ratio of CH_3Cl and perfluorohexane (PFH) for at least 2h to assess potential side reactions and unwanted losses of CH_3Cl. For the experiment with chlorine, this was done under dark conditions in the presence of 10 ppm Cl_2. For the OH experiments, this was either done in the absence of light or ozone. None of these tests revealed indication for a measurable loss of CH_3Cl and thus for any biasing side effects or reactions. In the methane degradation experiments CO_2 was used as an internal standard to correct for the methane mixing ratios for dilution. A blank experiment over 9h carried out with a dilution flow of 4 L min^{-1} of zero air revealed a slope (-0.00118±0.00001) $min^{-1}$for CH_4 loss and a slope of (0.00117±0.000007) min^{-1} for the CO_2 loss respectively.

This corresponds to a dilution flow of (4.1±0.1) L min-1 being in good agreement with the pre-set dilution flow (the major uncertainty in this calculation is the exact volume of the chamber). During this blank experiment, the dilution corrected mixing ratio of CH_4 changed by less than 0.2%.

In our study, photolysis of ozone (620 nmol mol^{-1} steady state mixing ratio) in the absence of water vapor (relative humidity <1%) but with 2000 µmol mol^{-1} H_2 (experiment 3) resulted in a CH_3Cl degradation of less than 3% over 10 hours and no measurable change in the isotopic composition of CH_3Cl. because of the insufficient OH yield.. The reaction rate constants of $O(^1D)$ with H_2 and H_2O at 298 K are $1.1*10^{-10}$ and $2.2*10^{-10}$ cm^3 $molecule^{-1}$ s^{-1} respectively (Burkholder et al.,2015). At a relative humidity of 70% (corresponding to 25000 ppm), the reaction with H_2O is by far the main pathway to form OH (with the H_2 pathway contributing less than 4% to the OH yield). This is consistent with the previous study, where ozone levels of 300 ppm were required for a sufficient OH production from H_2 (Gola et al., 2005; Sellevåg et al., 2006). For this experiment the OH lifetime of CH_3Cl can be estimated to about 330 h. In experiment four, where both CH_3Cl and CH_4 were present, the ratio of the measured rate constants for the reaction of CH_3Cl and CH_4 with OH was 5.8. This ratio agrees well with that of the recommended rate constants of 5.6 at 298 K ($6.3x10^{-15}$ cm3 s^{-1} for CH_4 and, $3.5x10^{-14}$ cm^3 s^{-1} for CH_3Cl at 298K; Burkholder et al., 2015).

The change in stable carbon isotope values of CH_3Cl ($\delta^{13}C(CH_3Cl)$) with extent of reaction and the corresponding Rayleigh plots of the CH_3Cl degradation experiments are shown in figure 1. The respective KIEs, derived from the slope of the Rayleigh plot, are summarized in table 2. For the reaction of CH_3Cl with OH, we determined a KIE of –(11.2±0.8) ‰ (n=3) and for the reaction with Cl we found a KIE of (-10.2±0.5) ‰ (n=1). The results from both laboratories generally agreed within ±1.5 ‰ (1σ) and showed no systematic difference. Variations in the initial mixing ratios (5 to 13 ppm) and isotopic composition ((-47.0±0.5) ‰ and (-40.3±0.5) ‰) of CH_3Cl in the OH experiments had no significant effect on the determination of the KIEs. Further, the increase in the light intensity and ozone mixing ratios in experiment four had no effect on the KIE.

The KIEs for the reaction of methane with OH and Cl, determined for validation purposes, agreed reasonable well with the previously published KIEs (Saueressig et al., 1995; 2001; Tyler et al., 2000; Feilberg et al., 2005). For the reaction of methane with OH we found a KIE of -4.7 ‰ being at the upper end of previous reported fractionation factors and for the reaction with Cl we found a KIE of -59‰ being more at the lower end of previously reported KIEs (table 3).

2.3 Discussion of the CH_3Cl degradation experiments

Our newly determined KIEs for the reaction of CH_3Cl with OH and Cl are five to six times smaller than the previous reported KIEs of (-59 ±10) ‰ for the reaction with OH and of (-70 ±10) ‰ for the reaction with Cl (Gola et al. 2005). In this section we first discuss potential sources of error in our study with particular respect to the differences between our study and the Gola study and then provide a more comprehensive comparison of our data with previous data. Gola et al. (2005) used a 250 l electro polished stainless steel chamber for their degradation experiments whereas used a 3500 smog chamber made from FEP foil, for the CH_3Cl degradation experiments. The large volume of our smog chamber may result in incomplete mixing and thus in an underestimation of the KIE due to transport limitation. The lifetime of CH_3Cl under the experimental conditions was in the order of 6 to 8h, whereas the turnover of air inside the chamber occurred on time scales of a few minutes - making incomplete mixing an unlikely source of error. Incomplete mixing would also have affected the determination of the respective KIEs for methane. With those values agreeing

well with previously reported KIEs we can exclude incomplete mixing as a potential source of error in our experiments. In the Gola et al. study the mixing ratios and isotope ratios with long path FTIR. In our study the mixing ratios were determined by GC-MS and the isotope ratios were measured by GC-IRMS in two different laboratories. Both labs used different analytical set ups, different sampling methods and different standards. However, the results from both labs generally agree within ±1.5‰ on the 1σ level and show no systematic difference. As outlined before different initial $\delta^{13}C(CH_3Cl)$ as well as different initial CH_3Cl mixing ratios had no significant effect on the determination of the KIEs. This makes analytical artefacts in our $\delta^{13}C$ determination unlikely. The Cl radical generation scheme was quite similar among both studies. Gola et al. (2005) used narrow band photolysis of Cl_2 employing a Philips TLD-08 flourescent lamp (λmax ~370) nm whereas we used broadband photolysis (300 to 700 nm) making this an unlikely source for the discrepancy in between the KIEs for the reaction of CH_3Cl with Cl.

In our study OH was generated via UV photolysis of ozone (steady state mixing ratios of 0.62 and 3.6 ppm) in the presence of water vapor (RH of 70%) and 2000 ppm H_2, whereas in the Gola study OH was generated in the absence of water vapor from the reaction of $O(^1D)$ with H_2 (2000 ppm) after UV-photolysis of ozone (300 ppm). Due to the much lower ozone mixing ratios employed in our study the OH generation in the absence of water vapor was not sufficient in our study. Both OH generation schemes are well established. However, Cantrell et al. (1990), who used UV-photolysis in the presence of water as an OH source, estimated that the reaction of CH_4 with $O(^1D)$ may contribute about 3% to the overall degradation. The higher ozone levels and the less efficient conversion of $O(^1D)$ to OH in the Gola et al. (2005) study suggest an overall higher transient $O(^1D)$ concentration as compared to our experiments. Anyhow, for CH_3Cl interferences from the reaction with $O(^1D)$ are less likely than for CH_4. The reaction rate for methane with $O(^1D)$ (1.7×10^{-10} cm^3 s^{-1}; Burkholder et al., 2015) is 2.7×10^4 times larger than the respective reaction rate for OH (6.3×10^{-15} cm^3 s^{-1}). In the case of CH_3Cl the ratio is only 7.4×10^3 (2.6×10^{-10} cm^3 s^{-1} and 3.5×10^{-14} cm^3 s^{-1}; Burkholder et al., 2015).

None of our tests prior each degradation experiment revealed indication for a measurable loss of CH_3Cl. In the CH_3Cl control experiment all experimental parameters beside the relative humidity and hence the OH yield were comparable to CH_3Cl degradation experiments with OH. The CH_3Cl loss of less than 3% over 10h and can be attributed to reaction with OH. Hence this experiment further confirms the absence of any biasing side reactions and we can safely exclude any measurable effect from potential side reactions on the determination of the KIEs in our study.

A comparison of our data with previously measured and calculated KIEs for the reaction of CH_3Cl methane and other VOCs with OH and Cl is provided in table 3. In a follow up study to Gola et al. (2005), Sellevåg et al. (2006) attributed these exceptionally large fractionation factors to higher internal barriers of rotation of the OH radical compared to the CH_4 + OH reaction. Using variational transition state theory, the authors calculated KIEs of -47 ‰ and -37 ‰ for the reaction of CH_3Cl with OH and Cl, respectively. However, a simultaneous theoretical study provided a KIE of only -3.6 ‰ for the reaction of CH_3Cl with OH (Jalili, & Akhavan, 2006). For C-H bond breakage, Streitwieser's semi-classical limit for isotope effects is -21 ‰ (Elsner et al., 2005) and for reactions involving hydrogen radical transfer, a KIE of -15‰, has been reported (Merrigan et al., 1990). Both values support a lower fractionation factor. For the reaction of ethane with OH that can be approximately regarded as a substituted methane a KIE of (-7.5±0.5) ‰ has been reported (Piansavan et al., 2017). One can estimate an upper limit for the reactive site by multiplying $\delta^{13}C$ with the number of carbon atoms in the molecule (Anderson et al., 2004). This leads to an upper limit of (-15.0±0.7) ‰ for the KIE at the reactive center. In line with this Anderson et al. (2004) reported a group kinetic isotope effect of –

(18.7±5.2) ‰ for the reaction of primary carbon atoms of alkanes with OH. The same group (Anderson et al., 2007) found a group kinetic isotope effect of (-18.6±0.3) ‰ for the respective reaction with Cl. Our smaller KIEs for the reaction of CH_3Cl with OH and Cl are much closer to these group specific KIEs than the previously reported ones of Gola et al. (2005).

To this end, the large discrepancy between our data and those of Gola et al. (2005) remains unresolved and cannot be explained from experimental details. However, the strongest support for our lower KIE arises from the absence of any significant seasonal variation in the tropospheric $\delta^{13}C(CH_3Cl)$, as outlined in section 3.2.

3 Carbon isotope modelling

3.1 Model set up

The model used in this study is similar to previous two box models (Tans, 1997; Sapart et al., 2012; Saltzman et al., 2004; Trudinger et al., 2004). The atmosphere is divided in two well-mixed semi hemispheric boxes, representing the northern, and the southern hemisphere and the interhemispheric exchange time is 360 days. The model simulates the major sources and sinks for both, the lighter ($^{12}CH_3Cl$) and the heavier isotopologue ($^{13}CH_3Cl$), as described by Sapart et al. (2012) for methane. The source and sink terms from the Xiao et al. model study (2010) serve as a starting point for our model. We use a simplified mass balance with four source categories having distinct isotopic source signatures: higher plants / unknown, oceans, biomass burning, and other known sources (table 4). Total net emissions were fixed at 4010 Gg a^{-1} with 2210 Gg a^{-1} in the northern hemisphere and 1800 Gg a^{-1} in the southern hemisphere. Losses are specified by pseudo first order rate coefficients. The sinks implemented in the model are losses due to the reaction with OH, losses to the surface ocean, losses to soils, and losses to the stratosphere (table 4). The seasonal source and sink terms are specified for each hemisphere using monthly means (Fig. 2). For each source category, the carbon isotope source signature was randomly varied within the given uncertainties. Seasonal variations were modeled with a time step of 1 day, using monthly averaged source and sink terms. Variations in the source composition were modeled with a time step of 90 days, using yearly averaged source and sink terms.

3.1.1 Sources

The ocean is treated as a net source for CH_3Cl with annual net emission of 335 Gg a^{-1} (range: 80 to 610 Gg a^{-1} (Hu et al., 2013). To account for the bidirectional nature of the gas exchange across the air/sea interface, net fluxes are broken down into unidirectional gross uptake and emission fluxes, with the uptake carrying the isotopic composition of the atmosphere and the emission carrying the isotopic information of the concurrent formation and degradation processes in the ocean. The gross uptake is calculated using an average transfer velocity of 17 cm h^{-1} for CO2 (Wanninkhof 2014) and a mean tropospheric mixing ratio of 540 pmol mol^{-1}. Gross emissions are then calculated as the difference between net emissions and gross uptake fluxes. The reader should note that this approach differs from that of Hu et al. (2013) and results in larger gross fluxes because gross fluxes are calculated for the entire ocean surface. In line with previous studies (Keppler et al. 2005), we estimate the average isotopic composition of dissolved CH_3Cl to (-36±6) ‰.

We applied a source strength of 910 Gg a^{-1} for biomass burning (range from 660 to 1230 Gg a^{-1}) with 68% originating from the northern hemisphere and the emissions peaking during hemispheric spring (Xiao et al., 2010). CH_3Cl from biomass burning shows a $\delta^{13}C$ of (-47±7) ‰ Czapiewski et al., 2002; Thompson et al., 2002).

The category "other known sources" comprises fungi wetlands and anthropogenic emissions with a total source strength of 365 Gg a^{-1} (range: 79 to 1016 Gg a^{-1}) and an averaged isotopic source signature of (-45.5±5.5) ‰ calculated from the source signatures given by Keppler et al. (2005). The emissions from the other known sources were constant over time with 16 Gg $month^{-1}$ in the northern hemisphere and 5.3 Gg $month^{-1}$ in the southern hemisphere.

The source category "Higher plants / missing" (900 to 3095 Gg a^{-1}) represents mainly emissions from the tropical rain forest (900 to 2650 Gg a^{-1}) with minor contributions from saltmarshes (80 to 160 Gg a^{-1}), rice paddies (5 Gg a^{-1}) and mangroves (~50 Gg a^{-1}). These emissions are almost equally distributed between both hemispheres and show a slight seasonal peak during hemispheric summer. In order to evaluate the emissions from higher plants, these emissions were divided into two fractions by introducing a split factor. The first fraction represents "true" emissions from higher plants, having an exceptionally depleted isotopic source signature of (-83±15) ‰ (Saito & Yokouchi, 2008; Saito et al., 2008). The second fraction represents an unknown or missing source. The $\delta^{13}C$ of this source is scaled to match the $\delta^{13}C$ of tropospheric CH_3Cl. A more depleted $\delta^{13}C$ for this source would point towards additional contributions from a lighter source, such as senescent leaf litter, whereas a more enriched $\delta^{13}C$ for this source points towards additional contributions from a more enriched source.

Saito et al. (2013) recently reported on the bidirectional exchange of CH_3Cl across the leaves of tropical plants with gross uptake rates being roughly $1/6^{th}$ of gross emission rates. The authors hypothesized that the gross uptake may be related to endosymbiotic bacteria. Because the incubation methods used in this study were the same as that previously used to determine the isotopic composition of CH_3Cl emitted from tropical plants (Saito & Yokouchi, 2008; Saito et al., 2008) we can reasonably assume that any isotopic effect of this bidirectional exchange is included in the previously reported carbon isotope ratios.

3.1.2 Sinks

The reaction with OH constitutes the single largest sink for CH_3Cl, accounting for approximately 80% of its removal from the troposphere. For this study, we used the OH-concentration fields from Spivakovsky et al. (2000) along with reaction rate constants of Burkholder et al. (2015) to derive monthly resolved lifetimes for both hemispheres. The lifetimes were then forced to reproduce seasonal variations of the mixing ratios at Mace Head in the northern hemisphere and at Cape Grim (Prinn et al., 2000), Tasmania, in the southern hemisphere. This resulted in a total tropospheric sink (OH + Cl) of 3614 Gg a^{-1}, being comparable to previous modeling studies (Xiao et al., 2010).

In most global budgets, soils are treated as a small sink for chloromethane of about ~250 Gg a^{-1}, though a larger uptake exceeding 1000 Gg a^{-1} has been suggested (Keppler et al., 2005; Carpenter et al., 2014). Based on Xiao et al. (2010), we a priori assumed a soil sink of 250 Gg a^{-1} with northern and southern hemispheric fractions of 180 and 70 Gg a^{-1}, respectively, reflecting the interhemispheric distribution of the land masses.

The microbial degradation of CH_3Cl in soils is assigned with a large carbon isotope fractionation of -47 ‰ (Miller et al., 2001; 2004). The only study, we are aware of, (Redeker et al., 2012) that investigates the isotopic composition of soil derived CH_3Cl reports a $\delta^{13}C$ of (-34±14) ‰. This suggests a substantially smaller apparent KIE for the soil uptake of CH_3Cl. The soil uptake of CH_3Cl can be regarded as a coupled diffusion reaction process, where CH_3Cl is first

transported into the soil and then undergoes microbial degradation. The apparent KIE of such coupled processes will depend on the KIEs of both steps and can be estimated from diffusion reaction models (Farquhar et al., 1981):

$$\varepsilon_{app} = \varepsilon_d + \frac{(\epsilon_m - \varepsilon_d) * (m_{d-m_m})}{m_d} \quad (4)$$

with ε_d and ε_m being the kinetic isotope effects assigned to microbial degradation (47‰) and diffusion (4‰) respectively. m_d is the total mass of CH_3Cl that enters the soil via diffusion and m_m represents the net soil sink.

The gross uptake flux (m_d) was estimated using a simple transfer resistance model along with the biomes and respective active seasons as previously used (Shorter et al., 1995). We used an overall atmospheric transfer resistance governing the transport to the soils surface (aerodynamic transport resistance, quasi-laminar sublayer resistance and in canopy transfer resistance) of 4 s/cm regardless of the biome that was derived from reported typical transfer resistances for different biomes (Zhang et al., 2003). The soil uptake is governed by molecular diffusion through the air filled spore space. The soil side transfer resistance can be estimated from the effective diffusion in the soil column. For a first rough estimate of the soil transfer resistance, we assume an air filled pore space of 0.3 (V/V) and a microbially inactive soil layer of 0.5 cm at the soil surface. Using the Penman model (Penman, 1940) and a diffusion coefficient of 0.144 cm^2s^{-1} in air, we obtain a soil transfer resistance of 17 s/cm. With a globally averaged transfer resistance of 21 s cm^{-1} and a CH_3Cl background concentration of 540 ppt and the land use categories from Shorter et al. (1995) we obtain an upper limit of 1300 Gg a^{-1} for m_d.

As depicted in figure 3, the apparent KIE of the soil uptake is bracketed by the kinetic isotope effect of both steps and decreases when increasing the net soil uptake The microbial degradation is rate limiting at low net uptake rates, and the apparent KIE of the soil uptake is close to that for microbial degradation. For instance, a soil sink of 250 Gg a^{-1} reveals an apparent KIE of -38‰. When the entire chloromethane diffusing into soils is microbially degraded, diffusion becomes the rate limiting step, and the apparent KIE matches that of diffusion.

In turn the imprint on the tropospheric $\delta^{13}C$ shows a parabolic distribution with a maximum at m_m = 0.5 m_d. The isolated effect of the soil sink would result in a maximum enrichment of 3.8‰ in the tropospheric $\delta^{13}C$ that reduces to 2.1‰ when accounting for the concurrent reduction in the OH sink. In this case, increasing the soil sink could even lead to a depletion in the tropospheric $\delta^{13}C$ once the apparent KIE of the soil sink becomes smaller than the KIE of the OH sink.

3.2 Modelled seasonal variations in the $\delta^{13}C$ of tropospheric CH_3Cl

Tropospheric CH_3Cl shows a pronounced seasonal cycle with an amplitude of 85 parts per trillion by volume (pptv) in northern hemispheric mid-latitudes (Prinn et al., 2000; Yoshida et al., 2006), reflecting the seasonality in the OH sink. This implies an inverse co-variation in the $\delta^{13}C$ of tropospheric CH_3Cl to an extent that is closely linked to the KIE of the OH sink. Our model nicely resembles mean tropospheric mixing ratios of about 539 pptv (Monzka et al., 2010; Carpenter et al, 2014) and the seasonal cycles of CH_3Cl in both hemispheres within ±4% (Fig. 4 upper panel). In our simulations, a KIE of -59‰ of the OH sink, produces an inverse co-variation of the $\delta^{13}C(CH_3Cl)$ with CH_3Cl mixing ratios with a seasonal amplitude of 9.2‰, whereas our new smaller KIE of -11.2 ‰ results in a seasonal amplitude of only 1.7‰ (Fig 4 lower panel). In both cases, random variations of ±10 ‰ in the isotopic source signatures, seasonal variations of the emission functions and variations in the soil sink resulted in a scatter of ±2 ‰

for the $\delta^{13}C$ of tropospheric CH_3Cl but did not significantly affect the differences in the seasonal amplitude of the $\delta^{13}C$ signal.

Most of the seasonal variation in the combined isotopic source signal (±4 ‰) is attenuated by the large tropospheric background, resulting in seasonal variations of the northern hemispheric $\delta^{13}C$ of less than ±1.1 ‰ attributable to the isotopic source signal. In a year round study carried out in Alert, Canada Thompson et al. (2002) found no clear correlation between the CH_3Cl mixing and isotope ratios. From their data the authors estimated the KIE for the OH sink being less than 5 ‰. As shown in figure 2 (lower panel) the seasonal variation in the tropospheric $\delta^{13}C(CH_3Cl)$ modelled with our KIE of -11.2‰ fit quite well to the measured variation given by Thompson et al. (2002). The lack of a significant co-variation between the mixing ratios and carbon isotope ratios was confirmed in second year round study (Rhew et al 2007). In sum the lacking covariation between the mixing ratios and carbon isotope ratios strongly supports our new KIE of -11.2‰ and make the previously reported larger KIEs highly unlikely.

3.3 Implications for the tropical rainforest source

A KIE of -59‰ for the OH sink requires a mean mass weighted isotopic source composition of -84.5 ‰ to balance the tropospheric $\delta^{13}C(CH_3Cl)$ of (-36.4±2.1) ‰ (Thompson et al., 2002), as shown in previous studies. Apart from large emissions from higher plants (Keppler et al., 2005; Saito & Yokouchi, 2008) in tropical rainforests, this KIE suggests additional substantial emissions from an even more depleted source, such as senescent leaf litter (Keppler et al., 2005; Saito & Yokouchi, 2008). In contrast, the revised smaller KIE of -11.2 ‰ requires a mean isotopic source signature of -48.5 ‰, being close to the mass weighted $\delta^{13}C$ of all other known sources excluding higher plants. Along with higher plant emissions of 2200 Gg a^{-1}, the new KIE of -11.2 ‰ yields a mean tropospheric $\delta^{13}C(CH_3Cl)$ of -56 ‰, being depleted by almost 20 ‰ in comparison to the mean reported tropospheric $\delta^{13}C(CH_3Cl)$.

We performed more than 10,000 steady state runs with random variations in the isotopic composition of tropospheric CH_3Cl (-36.4±2.1‰), the isotopic source signatures as indicated above and the KIE of the soil sink to assess the range of CH_3Cl-emissions from higher plants. The source category “Higher plants” was divided in two fractions, one representing “true” emissions from higher plants and the other representing missing emissions. The $\delta^{13}C$ of the missing emissions was always scaled to match the tropospheric $\delta^{13}C(CH_3Cl)$.

As shown in Figure 5, the strength of the tropical rainforest source is directly linked to the strength and isotopic composition of missing emissions. A tropical rainforest source of 600±200 Gg a^{-1} suggests missing emissions of (1400±200) Gg a^{-1}, requiring a $\delta^{13}C$ of (-45±6) ‰ to balance the tropospheric $\delta^{13}C(CH_3Cl)$. This $\delta^{13}C$ is close to the mean isotopic composition of all other known sources. Increasing the tropical rainforest source results in an equivalent reduction in missing emissions but requires a more enriched $\delta^{13}C$ for the missing emissions. For instance, balancing a tropical rainforest source of 1100±200 Gg a^{-1} requires missing emissions of the same magnitude having a $\delta^{13}C$ of -31±6‰. This is at the upper end of reported source signatures and may thus serve as a boundary to constrain the rainforest source from an isotopic perspective.

4 Carbon density based revision of the tropical rainforest source

Interestingly, support for our lower estimate arises from previous studies on the tropical rainforest CH_3Cl source when using above ground carbon density instead of coverage area for upscaling the CH_3Cl emission factors.

Large uncertainties in upscaling of local derived plant emissions to global scales can arise from i) temporal variations in the emissions, ii) spatial variability in environmental drivers, species composition and vegetation cover. Within the widely used FAO land cover classes, forests are defined as land with a tree cover exceeding 10%, a potential tree height of 5m and an area of at least 0.5 ha (FAO, 2012). Tropical rainforests encompass such sparsely covered areas with a carbon density of only a few Mg ha^{-1} (Asner et al., 2010; Pereira Junior et al., 2016) as well as very dense mature rainforests with a canopy height of more than 40 m and above ground carbon densities sometimes exceeding 300 Mg ha^{-1} (Kato et al, 1978). This suggests a large variability in biomass that cannot be assessed with the previously used area based upscaling approaches. Area based estimates may be improved by leaf area index or above ground carbon density based approaches. There is some indication that CH_3Cl is mainly emitted by mature trees (Saito & Yokouchi, 2008; Saito et al., 2008; 2013). This is more readily reflected by carbon density than by leaf area. Further the available carbon density data products allow a direct discrimination between tropical forests and other tropical vegetation. We thus propose a carbon density based upscaling approach of experimentally derived emission factors to reduce uncertainties arising from the spatial variability in above ground biomass. We first convert reported area based emission factors to carbon density based emission factors and then multiply them with the carbon stock of the tropical rainforest:

$$F(CH_3Cl) = \frac{E_F * C_{RF}}{C_{st}} \quad (5)$$

Here $F(CH_3Cl)$ is the source strength [Gg a^{-1}], E_F is the experimentally derived emission factor [Gg ha^{-1} a^{-1}], C_{st} is the above ground carbon density assigned to the sampling site [Gg ha^{-1}] and C_{RF} is the estimated total above ground biomass [Gg] of the respective biome, in this case the tropical rainforest.

The first direct evidence for strong CH_3Cl emissions from tropical plants came from branch incubations of tropical plants in a greenhouse (Yokouchi et al., 2000). This study revealed particularly high emission from dipterocarp species being dominant in tropical lowland rainforests of South and Southeast Asia, and suggested mean CH_3Cl emissions of 74 µg m^2h^{-1}. Several follow up studies carried out in tropical rainforests reported ten- to fivefold lower fluxes (Saito et al, 2008; 2013; Gebbhard et al., 2008; Blei et al., 2010). We exclude the high emission factor from the greenhouse study from our reanalysis of the tropical rainforest source and focus on the studies, providing experimentally derived emission factors for CH_3Cl emissions from tropical forests and allowing for a sufficient estimate of carbon densities assignable to them. Details on these studies are provided in table 5. Three studies have been carried out in lowland tropical rainforests of South East Asia, and one has been carried out over Surinam in South America. We are not aware of any CH_3Cl flux measurements from African tropical rainforests. Two studies relied on branch or leaf incubation to measure CH_3Cl fluxes (Saito et al, 2013; Blei et al., 2010). A third study used a micrometeorological approach and in addition performed leaf and branch incubation (Saito et al, 2008). The remaining study (Gebbhardt et al., 2008) derived CH_3Cl emissions factors from concentration gradients above the rainforest. The concentration gradients were obtained from canister samples taken at different heights above the rainforest from an airplane. The results from branch and leaf incubations were first normalized to leaf dry weight and then converted to area based emission factors using reported allometric data for Southeast Asian tropical lowland rainforests along with assumptions on the distribution and abundance of the investigated species. The mean area normalized fluxes (8.0 µg m^2 h^{-1} ±45%) from these studies show a notably larger variability than the original leaf biomass normalized fluxes (0.028 µg $g^{-1}h^{-1}$ ±10%), although all three studies referred to the same allometric data (Yamakura et al., 1986) in their conversion. Noteworthy, the study reporting the lowest emissions factors from branch enclosures reported almost three times higher fluxes using a

micrometeorological approach. In sum, the area based factors agree within a factor of 3 and ranged from 5.0 to 14 µg m^2h^{-1} (9.1 µg m^2h^{-1} ±37%).

The three south East Asian studies refer to a dense and mature dipterocarp forest with an above ground carbon density of (265±44) Mg C ha^{-1} (Yamakura et al., 1986) that we apply here. For the study carried out above the rainforest of Surinam, we derived a carbon density of (160±15) Mg ha^{-1} from carbon density maps (Saatchi et al., 2011; Baccini et al., 2012) .This range agrees with the FAO estimate for French Guyana (FAO, 2015) and is supported by several field surveys carried out in this region (Chave et al., 2001; 2008). With this, we obtain a mean carbon density based emission factor of (4.0±1.2) g Mg, referring to a mean carbon density of 202 Mg ha^{-1}. This is well above the average tropical rainforest carbon density, ranging from 96 to 117 Mg ha^{-1} (Bachini et al, 2012; Saatchi et al., 2011; Köhl et al., 2015; FAO, 2015).

In consequence, our carbon density based estimates of the tropical CH_3Cl source are 30 to 70% lower than the respective area based estimates (table 6). The difference is in the range of 30% for dense old grown evergreen forests such as the Tierra Firme forests of French Guyana, between 40% and 50% for the moist tropical rainforest, and increases to almost 70% for the entire pantropical forests including dry tropical forests, degraded forests and plantations. This trend reflects the decreasing trend in carbon density in the tropical rainforest biomes as well as the effect of forest degradation. Regardless of the source for the carbon density estimates, our approach suggests a tropical rainforest CH_3Cl source of (670±250) Gg a^{-1}, being 53% to 65% lower than the respective area based estimates n the range 1200 to 2000 Gg a^{-1} (Saito et al, 2008; 2013; Gebbhard et al., 2008; Blei et al., 2010).

The uncertainty in the area based emission factors is estimated to 24% from the standard deviation of the reported means. Additional uncertainties for our carbon density based upscaling (as compared to the previous area based upscaling) arise from the uncertainties in the total above ground carbon stocks (±8.6%) and the site specific carbon density (±15%). Using error propagation, we estimate the total uncertainty of our approach to ±30.4%.

5 Conclusions

We reported new KIEs for the reaction of CH_3Cl with OH and Cl of (-11.2±0.8) ‰ (n=3) and (-10.2±0.5) ‰ respectively being five to seven times smaller than the previous reported KIEs for these reactions. The cause for the large discrepancies remains unresolved. However, the strongest support for the reliability of our new fractionation factors arises from the absence of any significant co-variation in the mixing and carbon isotope ratios of tropospheric CH_3Cl.

Conjoining our new KIEs of the tropospheric CH_3Cl sinks and the biomass based upscaling of previously reported emission factors suggest a tropical vegetation source of only (670±210) Gg a^{-1}, being about threefold smaller than suggested in current budgets. We assign $\delta^{13}C$ of -45±6‰ to the missing emissions of (1530±190) Gg a^{-1}. Notably increasing the soil sink by 750 Gg a^{-1} and decreasing biomass burning emissions by 460 Gg a^{-1}, as suggested in the latest assessment on ozone depleting substances[3] would substantially increase this gap but have a negligible effect on the isotopic composition of the missing emissions. The $\delta^{13}C$ value of the missing emissions matches with the mean source signature of the other known sources (except rainforests). Increasing these emissions within the given ranges might reduce the gap to (1100±200) Gg a^{-1}. From a purely isotopic perspective, in particular larger emissions from

biomass burning could further reduce this gap. However, this is highly speculative as virtually any source combination providing a mean $\delta^{13}C$ of -45±6‰ could fill the gap.

With CH_3Cl being the single largest natural carrier of chlorine to the stratosphere, predicting future baselines of stratospheric chlorine require a better understanding of the global CH_3Cl cycle and an identification of the missing emissions.

Data availability. The data used in this publication and the model code are available to the community and can be accessed by request to the corresponding author.

Acknowledgements. We acknowledge the German Federal Ministry of Education and Research (BMBF) for funding within SOPRAN 'Surface Ocean Processes in the Anthropocene (grants 03F0611E and 03F0662E). This study was further supported by DFG (KE 884/ 8- 1; KE 884/8- 2, KE 884/ 10- 1) and by the DFG research unit 'Natural Halogenation Processes in the Environment - Atmosphere and Soil' (KE 884/7- 1, SCHO 286/7- 2, ZE 792/5 -2). We finally thank, S. O'Doherty, and P.J. Fraser for the AGAGE data from Mace Head and Cape Grim. AGAGE is supported principally by NASA (USA) grants to MIT and SIO, and also by: DECC (UK) and NOAA (USA) grants to Bristol University; CSIRO and BoM (Australia): FOEN grants to Empa (Switzerland); NILU (Norway); SNU (Korea); CMA (China); NIES (Japan); and Urbino University (Italy)

Author contributions E.B., F.K, J.W. and C.Z. designed the experiment, E.B, J.W and C.Z carried out the Smog chamber experiments. M.G carried out the isotope analysis in Heidelberg and E.B carried out the isotope analysis in Hamburg. E.B performed the modelling work. All authors contributed equally to the preparation of the manuscript.

6 References

Asner, G. P., Powell, G. V. N., Mascaro, J., Knapp, D. E., Clark, J. K., Jacobson, J., Kennedy-Bowdoin, T., Balaji, A., Paez-Acosta, G., Victoria, E., Secada, L., Valqui, M., and Hughes, R. F.: High-resolution forest carbon stocks and emissions in the Amazon, Proceedings of the National Academy of Sciences, 107, 16738-16742, 10.1073/pnas.1004875107, 2010.

Baccini, A., Goetz, S. J., Walker, W. S., Laporte, N. T., Sun, M., Sulla-Menashe, D., Hackler, J., Beck, P. S. A., Dubayah, R., Friedl, M. A., Samanta, S., and Houghton, R. A.: Estimated carbon dioxide emissions from tropical deforestation improved by carbon-density maps, Nature Climate Change, 2, 182, 10.1038/nclimate1354; https://www.nature.com/articles/nclimate1354#supplementary-information, 2012.

Bahlmann, E., Weinberg, I., Seifert, R., Tubbesing, C., and Michaelis, W.: A high volume sampling system for isotope determination of volatile halocarbons and hydrocarbons, Atmos. Meas. Tech., 4, 2073-2086, 10.5194/amt-4-2073-2011, 2011.

Blei, E., Hardacre, C. J., Mills, G. P., Heal, K. V., and Heal, M. R.: Identification and quantification of methyl halide sources in a lowland tropical rainforest, Atmospheric Environment, 44, 1005-1010, https://doi.org/10.1016/j.atmosenv.2009.12.023, 2010.

J. B. Burkholder, Sander, S. P., Abbatt, J., Barker, J. R., Huie, R. E., Kolb, C. E., Kurylo, M. J., Orkin, V. L., Wilmouth, D.M. and Wine, P. H.: Chemical Kinetics and Photochemical Data for Use in Atmospheric Studies, Evaluation No. 18," JPL Publication 15-10, Jet Propulsion Laboratory, Pasadena, 2015.

Butler, J. H.: Better budgets for methyl halides?, Nature, 403, 260, 10.1038/35002232, 2000.

Carpenter, L. J., Reimann, S., Burkholder, J. B., Clerbaux, C., Hall, B., Hossaini, R., Laube, J., and Yvon-Lewis, S.: Chapter 1: Update on Ozone-Depleting Substances (ODSs) and Other Gases of Interest to the Montreal Protocol, in: Scientific Assessment of Ozone Depletion, Global Ozone Research and Monitoring Project Report,World Meteorological Organization (WMO), 21– 125, 2014.

Chave, J., RiÉRa, B., and Dubois, M.-A.: Estimation of biomass in a neotropical forest of French Guiana: spatial and temporal variability, Journal of Tropical Ecology, 17, 79-96, 10.1017/S0266467401001055, 2001.

Chave, J., Olivier, J., Bongers, F., Châtelet, P., Forget, P.-M., van der Meer, P., Norden, N., Riéra, B., and Charles-Dominique, P.: Above-ground biomass and productivity in a rain forest of eastern South America, Journal of Tropical Ecology, 24, 355-366, 10.1017/S0266467408005075, 2008.

Czapiewski, K. v., Czuba, E., Huang, L., Ernst, D., Norman, A. L., Koppmann, R., and Rudolph, J.: Isotopic Composition of Non-Methane Hydrocarbons in Emissions from Biomass Burning, Journal of Atmospheric Chemistry, 43, 45-60, 10.1023/a:1016105030624, 2002.

Danzer, K., Wagner, M. and Fischbacher, C.: Calibration by orthogonal and common least squares – Theoretical and practical aspects, Fresenius J Anal Chem 352, 407-412, 1995

DeMore, W. B.: Rate constant ratio for the reactions of hydroxyl with methane-d and methane, The Journal of Physical Chemistry, 97, 8564-8566, 10.1021/j100135a006, 1993.

Elsner, M., Zwank, L., Hunkeler, D., and Schwarzenbach, R. P.: A New Concept Linking Observable Stable Isotope Fractionation to Transformation Pathways of Organic Pollutants, Environmental Science & Technology, 39, 6896-6916, 10.1021/es0504587, 2005.

Farquhar, G., O'Leary, M., and Berry, J.: On the Relationship Between Carbon Isotope Discrimination and the Intercellular Carbon Dioxide Concentration in Leaves, Functional Plant Biology, 9, 121-137, https://doi.org/10.1071/PP9820121, 1982.

Feilberg, K. L., Griffith, D. W. T., Johnson, M. S., and Nielsen, C. J.: The 13C and D kinetic isotope effects in the reaction of CH4 with Cl, International Journal of Chemical Kinetics, 37, 110-118, 10.1002/kin.20058, 2005.

Gebhardt, S., Colomb, A., Hofmann, R., Williams, J., and Lelieveld, J.: Halogenated organic species over the tropical South American rainforest, Atmos. Chem. Phys., 8, 3185-3197, 10.5194/acp-8-3185-2008, 2008.

Gola, A. A., D'Anna, B., Feilberg, K. L., Sellevåg, S. R., Bache-Andreassen, L., and Nielsen, C. J.: Kinetic isotope effects in the gas phase reactions of OH and Cl with CH₃Cl, CD₃Cl, and ¹³CH₃Cl, Atmos. Chem. Phys., 5, 2395-2402, 10.5194/acp-5-2395-2005, 2005.

Greule, M., Huber, S. G., and Keppler, F.: Stable hydrogen-isotope analysis of methyl chloride emitted from heated halophytic plants, Atmos. Environ., 62, 584-592, 10.1016/j.atmosenv.2012.09.007, 2013.

Hu, L., Yvon-Lewis, S. A., Butler, J. H., Lobert, J. M., and King, D. B.: An improved oceanic budget for methyl chloride, Journal of Geophysical Research: Oceans, 118, 715-725, doi:10.1029/2012JC008196, 2013.

Jalili, S. and Akhavan, M.: The study of isotope effects of chloroform and chloromethane using vibrational frequencies, Journal of Molecular Structure, Theochem 765, 105-114, 10.1016/j.theochem.2006.03.011, 2006.

Kato, R., Tadaki Y. and Ogawa, H.: Plant biomass and growth increment studies in Pasoh Forest, *Malay. Nat. J.* **30** (2), 211-224. 1978.

Keppler, F., Harper, D. B., Röckmann, T., Moore, R. M., and Hamilton, J. T. G.: New insight into the atmospheric chloromethane budget gained using stable carbon isotope ratios, Atmos. Chem. Phys., 5, 2403-2411, 10.5194/acp-5-2403-2005, 2005.

Keppler, F., Bahlmann, E., Greule, M., Schöler, H. F., Wittmer, J., and Zetzsch, C.: Mass spectrometric measurement of hydrogen isotope fractionation for the reactions of chloromethane with OH and Cl, Atmos. Chem. Phys., 18, 6625-6635, 10.5194/acp-18-6625-2018, 2018.

Köhl, M., Lasco, R., Cifuentes, M., Jonsson, Ö., Korhonen, K. T., Mundhenk, P., de Jesus Navar, J., and Stinson, G.: Changes in forest production, biomass and carbon: Results from the 2015 UN FAO Global Forest Resource Assessment, Forest Ecology and Management, 352, 21-34, https://doi.org/10.1016/j.foreco.2015.05.036, 2015.

Merrigan, S. R., Le Gloahec, V. N., Smith, J. A., Barton, D. H. R. and Singleton, D. A.: Separation of the primary and secondary kinetic isotope effects at a reactive center using starting material reactivities. Application to the $FeCl_3$-catalyzed oxidation of C-H bonds with tert-butyl hydroperoxide. Tetrahedron Lett. 40, 3847-3850. 1990.

Miller, L. G., Kalin, R. M., McCauley, S. E., Hamilton, J. T. G., Harper, D. B., Millet, D. B., Oremland, R. S., and Goldstein, A. H.: Large carbon isotope fractionation associated with oxidation of methyl halides by methylotrophic bacteria, Proceedings of the National Academy of Sciences, 98, 5833-5837, 10.1073/pnas.101129798, 2001.

Miller, L. G., Warner, K. L., Baesman, S. M., et al.: Degradation of methyl bromide and methyl chloride in soil microcosms: Use of stable C isotope fractionation and stable isotope probing to identify reactions and the responsible microorganisms, Geochim. Cosmochim. Acta, 68, 3271–3283, 2004.

Monzka, S.A., Reimann, S. et al.,: Chapter 1: Ozone-Depleting Substances (ODSs) and Other Gases of Interest to the Montreal Protocol, in: Scientific Assessment of Ozone Depletion, Global Ozone Research and Monitoring Project Report, World Meteorological Organization (WMO) Report 52, 2010.

Penman, H. L.: Gas and vapour movements in the soil: I. The diffusion of vapours through porous solids, The Journal of Agricultural Science, 30, 437-462, 10.1017/S0021859600048164, 2009.

Pereira Júnior, L. R. et al. Carbon stocks in a tropical dry forest in Brazil. *Revista Ciência Agronômica* **47**, 32-40 2016.

Piansawan, T., Saccon, M., Vereecken, L., Gensch, I., and Kiendler-Scharr, A.: Temperature dependence of stable carbon kinetic isotope effect for the oxidation reaction of ethane by OH radicals: Experimental and theoretical studies, Journal of Geophysical Research: Atmospheres, 122, 8310-8324, doi:10.1002/2017JD026950, 2017.

Prinn, R. G., Weiss, R. F., Fraser, P. J., Simmonds, P. G., Cunnold, D. M., Alyea, F. N., O'Doherty, S., Salameh, P., Miller, B. R., Huang, J., Wang, R. H. J., Hartley, D. E., Harth, C., Steele, L. P., Sturrock, G., Midgley, P. M., and McCulloch, A.: A history of chemically and radiatively important gases in air deduced from ALE/GAGE/AGAGE, Journal of Geophysical Research: Atmospheres, 105, 17751-17792, doi:10.1029/2000JD900141, 2000; http://agage.mit.edu/data, last visited 11.15.2017

Redeker, K. R., Davis, S., and Kalin, R. M.: Isotope values of atmospheric halocarbons and hydrocarbons from Irish urban, rural, and marine locations, Journal of Geophysical Research: Atmospheres, 112, doi:10.1029/2006JD007784, 2007.

Redeker, K. R., and Kalin, R. M.: Methyl chloride isotopic signatures from Irish forest soils and a comparison between abiotic and biogenic methyl halide soil fluxes, Global Change Biology, 18, 1453-1467, doi:10.1111/j.1365-2486.2011.02600.x, 2012.

Rhew, R. C., Miller, B. R., Bill, M., Goldstein, A. H., and Weiss, R. F.: Environmental and biological controls on methyl halide emissions from southern California coastal salt marshes, Biogeochemistry, 60, 141-161, 10.1023/a:1019812006560, 2002.

Rudolph, J., Czuba, E., and Huang, L.: The stable carbon isotope fractionation for reactions of selected hydrocarbons with OH-radicals and its relevance for atmospheric chemistry, Journal of Geophysical Research: Atmospheres, 105, 29329-29346, doi:10.1029/2000JD900447, 2000.

SAATCHI, S. S., HOUGHTON, R. A., DOS SANTOS ALVALÁ, R. C., SOARES, J. V., and YU, Y.: Distribution of aboveground live biomass in the Amazon basin, Global Change Biology, 13, 816-837, doi:10.1111/j.1365-2486.2007.01323.x, 2007.

Saatchi, S. S., Harris, N. L., Brown, S., Lefsky, M., Mitchard, E. T. A., Salas, W., Zutta, B. R., Buermann, W., Lewis, S. L., Hagen, S., Petrova, S., White, L., Silman, M., and Morel, A.: Benchmark map of forest carbon stocks in tropical regions across three continents, Proceedings of the National Academy of Sciences, 108, 9899-9904, 10.1073/pnas.1019576108, 2011.

Saito, T., and Yokouchi, Y.: Stable carbon isotope ratio of methyl chloride emitted from glasshouse-grown tropical plants and its implication for the global methyl chloride budget, Geophysical Research Letters, 35, doi:10.1029/2007GL032736, 2008.

Saito, T., Yokouchi, Y., Kosugi, Y., Tani, M., Philip, E., and Okuda, T.: Methyl chloride and isoprene emissions from tropical rain forest in Southeast Asia, Geophysical Research Letters, 35, doi:10.1029/2008GL035241, 2008.

Saito, T., Yokouchi, Y., Phillip, E., and Okuda, T.: Bidirectional exchange of methyl halides between tropical plants and the atmosphere, Geophysical Research Letters, 40, 5300-5304, doi:10.1002/grl.50997, 2013.

Saltzman, E. S., Aydin, M., De Bruyn, W. J., King, D. B., and Yvon-Lewis, S. A.: Methyl bromide in preindustrial air: Measurements from an Antarctic ice core, Journal of Geophysical Research: Atmospheres, 109, doi:10.1029/2003JD004157, 2004.

Sapart, C. J., Monteil, G., Prokopiou, M., van de Wal, R. S. W., Kaplan, J. O., Sperlich, P., Krumhardt, K. M., van der Veen, C., Houweling, S., Krol, M. C., Blunier, T., Sowers, T., Martinerie, P., Witrant, E., Dahl-Jensen, D., and Röckmann, T.: Natural and anthropogenic variations in methane sources during the past two millennia, Nature, 490, 85, 10.1038/nature11461
https://www.nature.com/articles/nature11461#supplementary-information, 2012.

Saueressig, G., Bergamaschi, P., Crowley, J. N., Fischer, H., and Harris, G. W.: Carbon kinetic isotope effect in the reaction of CH4 with Cl atoms, Geophysical Research Letters, 22, 1225-1228, doi:10.1029/95GL00881, 1995.

Saueressig, G., Crowley, J. N., Bergamaschi, P., Brühl, C., Brenninkmeijer, C. A. M., and Fischer, H.: Carbon 13 and D kinetic isotope effects in the reactions of CH4 with O(1 D) and OH: New laboratory measurements and their implications for the isotopic composition of stratospheric methane, Journal of Geophysical Research: Atmospheres, 106, 23127-23138, doi:10.1029/2000JD000120, 2001.

Sellevåg, S. R., Nyman, G., and Nielsen, C. J.: Study of the Carbon-13 and Deuterium Kinetic Isotope Effects in the Cl and OH Reactions of CH4 and CH3Cl, The Journal of Physical Chemistry A, 110, 141-152, 10.1021/jp0549778, 2006.

Shorter, J. H., Kolb, C. E., Crill, P. M., Kerwin, R. A., Talbot, R. W., Hines, M. E., and Harriss, R. C.: Rapid degradation of atmospheric methyl bromide in soils, Nature, 377, 717, 10.1038/377717a0, 1995.

Spivakovsky, C. M., Logan, J. A., Montzka, S. A., Balkanski, Y. J., Foreman-Fowler, M., Jones, D. B. A., Horowitz, L. W., Fusco, A. C., Brenninkmeijer, C. A. M., Prather, M. J., Wofsy, S. C., and McElroy, M. B.: Three-dimensional climatological distribution of tropospheric OH: Update and evaluation, Journal of Geophysical Research: Atmospheres, 105, 8931-8980, doi:10.1029/1999JD901006, 2000.

Tans, P. P.: A note on isotopic ratios and the global atmospheric methane budget, Global Biogeochemical Cycles, 11, 77-81, doi:10.1029/96GB03940, 1997.

Thompson, A. E., Anderson, R. S., Rudolph, J., and Huang, L.: Stable carbon isotope signatures of background tropospheric chloromethane and CFC113, Biogeochemistry, 60, 191-211, 10.1023/a:1019820208377, 2002.

Trudinger, C. M., Etheridge, D. M., Sturrock, G. A., Fraser, P. J., Krummel, P. B., and McCulloch, A.: Atmospheric histories of halocarbons from analysis of Antarctic firn air: Methyl bromide, methyl chloride, chloroform, and dichloromethane, Journal of Geophysical Research: Atmospheres, 109, doi:10.1029/2004JD004932, 2004.

Tyler, S. C., Ajie, H. O., Rice, A. L., Cicerone, R. J., and Tuazon, E. C.: Experimentally determined kinetic isotope effects in the reaction of CH4 with Cl: Implications for atmospheric CH4, Geophysical Research Letters, 27, 1715-1718, doi:10.1029/1999GL011168, 2000.

Wanninkhof, R.: Relationship between wind speed and gas exchange overthe ocean revisited. Limnology and Oceanography: Methods 12, 351-362, 10.4319/lom.2014.12.351, 2014.

Wittmer, J., Bleicher, S., and Zetzsch, C.: Iron(III)-Induced Activation of Chloride and Bromide from Modeled Salt Pans, The Journal of Physical Chemistry A, 119, 4373-4385, 10.1021/jp508006s, 2015.

Xiao, X., Prinn, R. G., Fraser, P. J., Weiss, R. F., Simmonds, P. G., O'Doherty, S., Miller, B. R., Salameh, P. K., Harth, C. M., Krummel, P. B., Golombek, A., Porter, L. W., Butler, J. H., Elkins, J. W., Dutton, G. S., Hall, B. D., Steele, L. P., Wang, R. H. J., and Cunnold, D. M.: Atmospheric three-dimensional inverse modeling of regional industrial emissions and global oceanic uptake of carbon tetrachloride, Atmos. Chem. Phys., 10, 10421-10434, 10.5194/acp-10-10421-2010, 2010.

Yamakura, T., Hagihara, A., Sukardjo, S., and Ogawa, H.: Aboveground biomass of tropical rain forest stands in Indonesian Borneo, Vegetatio, 68, 71-82, 10.1007/bf00045057, 1986.

Yokouchi, Y., Noijiri, Y., Barrie, L. A., Toom-Sauntry, D., Machida, T., Inuzuka, Y., Akimoto, H., Li, H. J., Fujinuma, Y., and Aoki, S.: A strong source of methyl chloride to the atmosphere from tropical coastal land, Nature, 403, 295, 10.1038/35002049, 2000.

Yoshida, Y., Wang, Y., Shim, C., Cunnold, D., Blake, D. R., and Dutton, G. S.: Inverse modeling of the global methyl chloride sources, Journal of Geophysical Research: Atmospheres, 111, doi:10.1029/2005JD006696, 2006.

Zhang, L., Brook, J. R., and Vet, R.: A revised parameterization for gaseous dry deposition in air-quality models, Atmos. Chem. Phys., 3, 2067-2082, 10.5194/acp-3-2067-2003, 2003.

Atmos. Chem. Phys. Discuss., https://doi.org/10.5194/acp-2018-855
Manuscript under review for journal Atmos. Chem. Phys.
Discussion started: 11 September 2018

Atmospheric Chemistry and Physics Discussions

7 Tables

Table 1: Experimental conditions of the degradation experiments with OH. The O3 mixing ratios are average steady state mixing ratios throughout the experiment, the Cl_2 mixing ratios refer to the initial mixing ratios at the beginning of each photolysis sequence.

Exp.	reactant		oxidant	O_3 Cl_2	Irridiation	H_2	rel. Hum.	T	OH
		ppmv		ppmv		ppmv	%	°C	cm^{-3}
1 &2	CH_3Cl	5 , 10	OH	0.62	1x55W, λ_{max} = 254 nm	2000	65	20.7	2.9 x 10^9
3	CH_3Cl	0.13	OH	0.62	1x55W, λ_{max} = 254 nm	2000	< 1	20.6	8.7 x 10^7
4	CH_3Cl, CH_4	13, 5	OH	3.7	4x55W, λ_{max} = 254 nm	2000	65	20.4	1.6 x 10^{10}
5	CH_4	5		0	4x55W, λ_{max} = 254 nm		72	20.3	
6	CH_4	6	OH	3.7	4x55W, λ_{max} = 254 nm		72 to 75	20.3	1.6 x 10^{10}
7	CH_3Cl	10	Cl	2 to 10	7x1200W 300 - 700 nm		< 1	20.7	
8	CH_4	5	Cl	2 to 10	7x1200W 300 - 700 nm		< 1	20.5	

Atmos. Chem. Phys. Discuss., https://doi.org/10.5194/acp-2018-855
Manuscript under review for journal Atmos. Chem. Phys.
Discussion started: 11 September 2018

Atmospheric Chemistry and Physics Discussions

Table 2: Summary of the kinetic isotope effects for the reaction of CH_3Cl and CH_4 with OH and Cl from this study. We used orthogonal regression to calculate ε and the respective uncertainties on the 1σ level for each experiment. In experiment 4 the ε for methane has not been determined.

		Hamburg		Heidelberg	
		ε	R^2	ε	R^2
Exp. 1	CH_3Cl +OH	-12.1 ± 0.6	0.95	-11.7 ± 0.4	0.99
Exp. 2		-12,1 ± 0.3	0.99	-10.5 ± 0.3	0.99
Exp. 4		-10.4 ± 0.4	0.99	-10.6 ± 0,6	0.99
Exp. 7	CH_3Cl + Cl	-10.3 ± 0.7	0.96	-10.4 ± 0.4	0.98
Exp. 5	CH_4 + OH			-4.7 ± 0.2	0.99
Exp. 8	CH_4 + Cl			-59.0 ± 1.3	0.99

Table 3: Compilation of kinetic isotope effects for the reaction of CH_3Cl, CH_4 and alkanes with OH and Cl

Reaction		ε	Method	Reference
CH_3Cl	+ OH	-58 ± 10	Smog chamber; O_3+H_2+hv (254 nm), FTIR	Gola et al., 2005
		-44	theoretical at 298K	Feilberg et al., 2005
		-3.6	theoretical	Jalili, S. & Akhavan, 2006
		-5 ± 3	derived from field data	Thompson et al., 2002
		-11.2 ± 0.8	**Smog Chamber; O_3+H_2O+hv (254 nm), GC-IRMS**	**This study**
CH_3Cl	+ Cl	-70 ± 10	Smog chamber; Cl+hv (370 nm), FTIR	Gola et al., 2005
		-35	theoretical at 298K	Feilberg et al., 2005
		-10.4 ± 0.5	**Smog Chamber; Cl_2+hv GC-IRMS**	**This study**
CH_4	+ OH	-3.9 ± 0.4	photo reactor; H_2O_2+hv, GC-IRMS	Saueressig et al. 2001
		-4.7 ± 0.2	**Smog Chamber; O_3+H_2O+hv (254 nm), GC-IRMS**	**This study**
CH_4	+ Cl	-58 ± 2	Smog chamber; Cl_2+hv FTIR	Sellevåg et al., 2006
		-66 ± 2	photo reactor; Cl_2+hv; TDLAS	Saueressig et al., 1995
		-62 ± 0.1	Smog Chamber; Cl_2+hv; DI-IRMS	Tyler et al., 2000
		-59	**Smog Chamber; Cl_2+hv GC-IRMS**	**This study**
C_2H_6	+ OH	-7.5 ± 0.5	reaction chamber; H_2O_2 + hv; GC-IRMS	Piansawan et al., 2017
R-**CH_3**	+ OH	-18.7 ± 5.2	reaction chamber; R-NO_2, NO + hv; GC-IRMS	Anderson et al., 2004
R-**CH_3**	+ Cl	-18.6 ± 0.3	reaction chamber; Cl_2 + hv; GC-IRMS	Anderson et al. 2007

Atmos. Chem. Phys. Discuss., https://doi.org/10.5194/acp-2018-855
Manuscript under review for journal Atmos. Chem. Phys.
Discussion started: 11 September 2018

Atmospheric Chemistry and Physics Discussions

Table 4: Simplified CH_3Cl source and sink scheme used in the model

	strength [Gg a^{-1}]			$\delta^{13}C$ (source) / ε (sink) [‰]		
sources	**best**	**range**		**best**	**range**	
Biomass burning	910	655 -	1125	-47	-40 -	-52
Oceans	335	210 -	480	-36	-31 -	-41
Higher Plants / unknown	2400	0 -	3095	-83	-70 -	-96
Other known sources	365	79 -	1016	-45	-40 -	-50
sinks						
OH, Cl	3614	3564 -	3000	-12 / -59		
soils*	250	200 -	1000	-37	-46 -	-2
stratosphere	146			0		

* The apparent KIE of the soil sink depends on its strength. See text for more details

Table 5: Calculation of carbon density based CH_3Cl emission factors from previously reported area based emission factors.

Site	**Method**	**Carbon density**	**Emission per**				**Ref.**
			leaf dry mass	**area**		**Carbon density**	
		Mg ha^{-1}	µg $g^{-1}h^{-1}$	µg m^{-2} h^{-1}	g ha^{-2} a^{-1}	g Mg^{-1}	
Glass house, Japan	branch enclosure	325	0.32	74,0			Yokouchi et al., 2000
Pasoh Forest Reserve, Malaysia	micrometerological	265		14,0	1226	4.6	Saito et al., 2013
	branch enclosure		0.03	5,0			
Pasoh Forest Reserve, Malaysia	branch enclosure	265	0.026	7,0	615	2.3	Saito et al., 2013
Danum Valley, Borneo	branch enclosure	265	0.03	12,0	1051	4	Blei et al., 2010
Borneo							
Surinam, French Guyana	gradient above canopy	160		9,5	832	5.2	Gebhardt et al., 2008
mean					**931**	**4**	
SD					**265**	**1.2**	

Atmos. Chem. Phys. Discuss., https://doi.org/10.5194/acp-2018-855
Manuscript under review for journal Atmos. Chem. Phys.
Discussion started: 11 September 2018

Atmospheric Chemistry and Physics Discussions

Table 6: Comparison of calculated area based and carbon density based emissions from tropical forests

Region	Area	C density	Area based			Carbon density based			
	10^6 ha	10^6 g ha^{-1}	Gg a^{-1}			Gg a^{-1}			% of area based
Brazil	586	112 [1]	496	±	143	247	±	73	50
Indonesia	165	112 [1]	140	±	40	69	±	20	50
Congo	205	92 [1]	173	±	50	71	±	21	41
Trop. Africa	775	62 [1]	655		189	182	±	53	28
Trop America	1209	77 [1]	1022		295	356	±	103	35
Trop Asia	474	98 [1]	401		116	176	±	51	44
Pantropics	**2458**	**78 [1]**	**2079**	**±**	**601**	**720**	**±**	**212**	**35**
Trop. Africa	393	82 [2]	332	±	96	121	±	36	36
Trop America	788	116 [2]	666	±	192	343	±	101	52
Trop Asia	289	119 [2]	244	±	71	129	±	38	53
Pantropics	**1470**	**105 [2]**	**1243**	**±**	**359**	**580**	**±**	**171**	**47**

[1] Saatchi et al. , 2011; [2] Bacchini et al., 2012

Atmos. Chem. Phys. Discuss., https://doi.org/10.5194/acp-2018-855
Manuscript under review for journal Atmos. Chem. Phys.
Discussion started: 11 September 2018

Atmospheric Chemistry and Physics Discussions

8 Figures

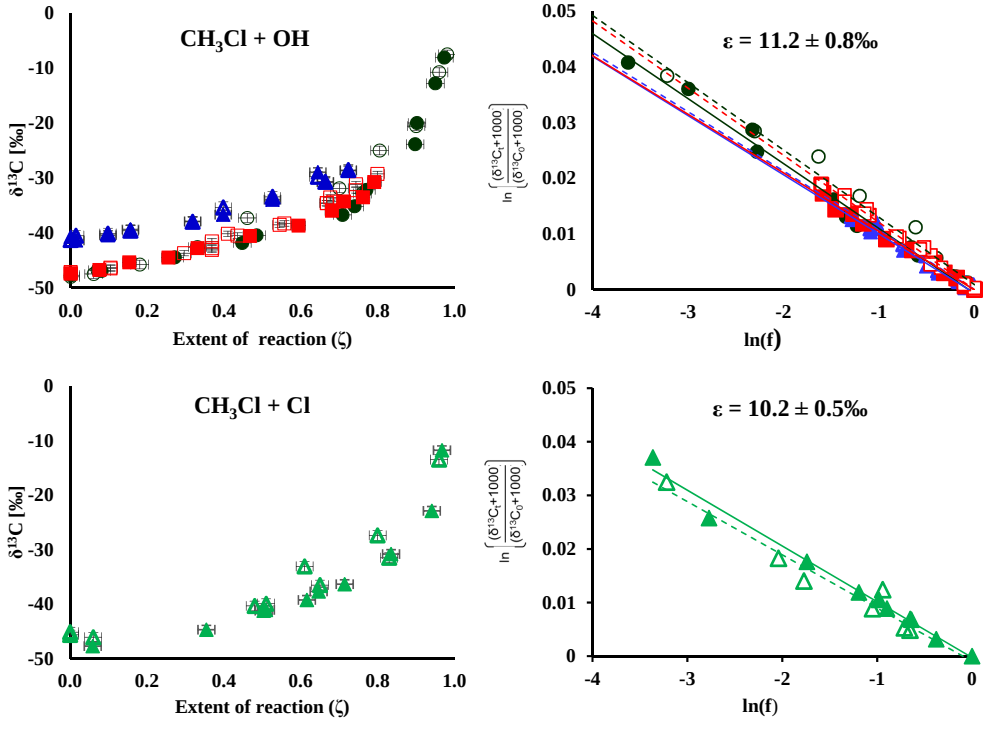

Figure 1: Change in $\delta^{13}C$ over extent of reaction (left hand side) and corresponding Rayleigh plots (right hand) from the CH_3Cl degradation experiments. Filled symbols and regression lines refer to the data from Heidelberg, open symbols and dashed regression lines show data from Hamburg. The colors refer to different degradation experiments (black: experiment 1; red: experiment 2, blue: experiment 4 and green experiment 7) . Errors in ζ were ±2% on the 1σ level. Errors in $\delta^{13}C$, as derived from the regression analysis, ranged from ±0.4 to ±1.4‰ on the 1σ level.

Atmos. Chem. Phys. Discuss., https://doi.org/10.5194/acp-2018-855
Manuscript under review for journal Atmos. Chem. Phys.
Discussion started: 11 September 2018

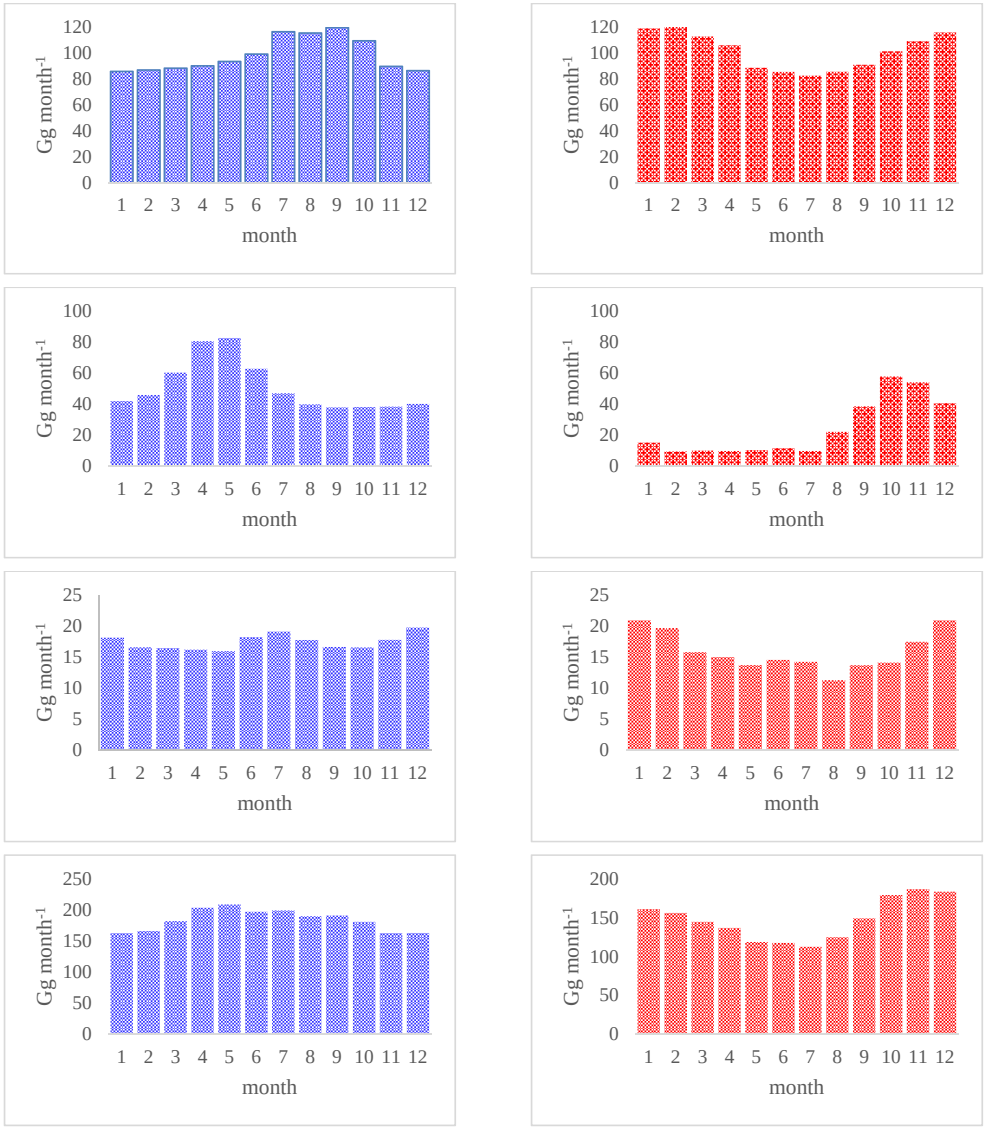

Figure 2: Chloromethane emissions in Gg month^{-1} for the northern (left side) and southern hemisphere (left side) Upper row panel: Combined emissions from higher plants and the unknown source; second row panel: biomass burning, third row panel: ocean net emission fluxes, fourth row panel total emissions. The emissions from the other known sources are constant over time with 16.6 Gg month^{-1} in the northern hemisphere and 5.8 Gg month^{-1} in the southern hemisphere.

Atmos. Chem. Phys. Discuss., https://doi.org/10.5194/acp-2018-855
Manuscript under review for journal Atmos. Chem. Phys.
Discussion started: 11 September 2018

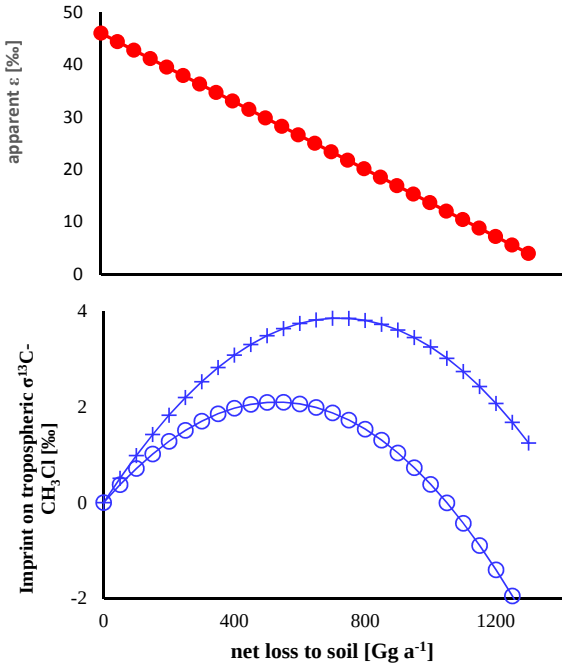

Figure 3: The upper panel shows the apparent ε of the soil sink versus the sink strength. The lower panel shows the resulting effect on tropospheric $\delta^{13}C$. Crosses show the pure effect e.g. in the absence of any other fractionating sink. Open circles show the resulting effect with an ε of -11.2‰ assigned to the OH sink.

Atmos. Chem. Phys. Discuss., https://doi.org/10.5194/acp-2018-855
Manuscript under review for journal Atmos. Chem. Phys.
Discussion started: 11 September 2018

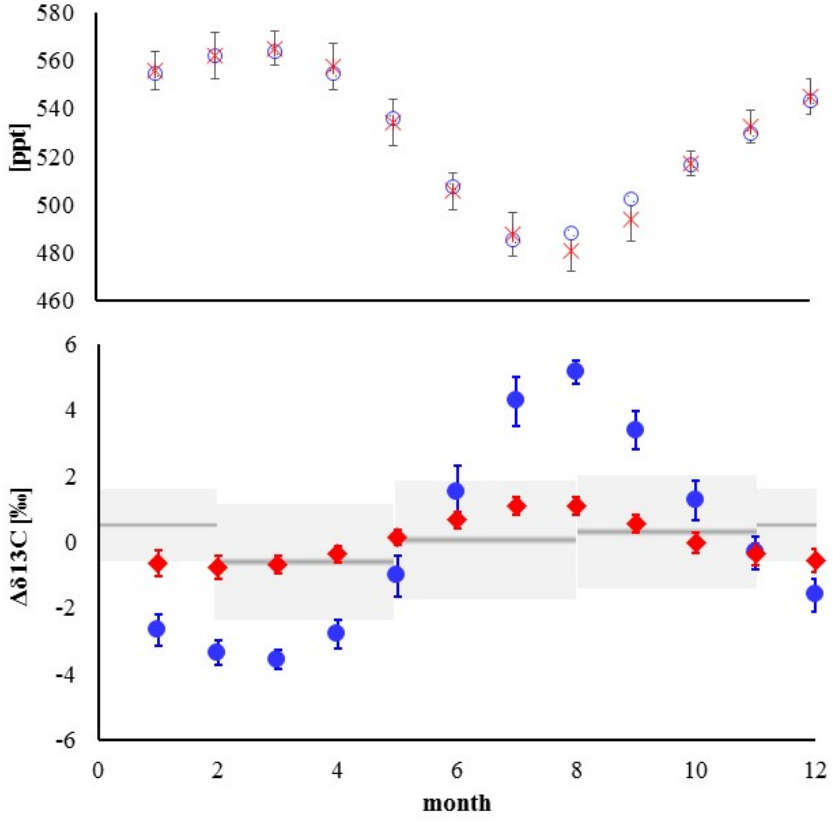

Figure 4: Upper panel: Comparison of modeled Northern hemispheric mixing ratios (blue open diamonds) with measured mixing ratios at Mace Head, Ireland (red crosses) for the period from 2004 to 2014 (Prinn et al., 2000). Error bars indicate the variations in the monthly means on the 1 σ level. Lower panel: Modeled seasonal fluctuations in the $\delta^{13}C$ of northern hemispheric CH_3Cl using an ε of -11.2‰ (red filled diamonds) and an ε of -59‰ (blue filled dots) as reportedd by Gola et al. (2005). The panel shows monthly averages from a 10-year simulation. The error bars indicate uncertainties (±1σ) from monthly random variations in the $\delta^{13}C$ of each source category as indicated in the text. The grey shaded area shows reported seasonal variations (seasonal mean ± 1σ) from Thompson et al. (2002).

Atmos. Chem. Phys. Discuss., https://doi.org/10.5194/acp-2018-855
Manuscript under review for journal Atmos. Chem. Phys.
Discussion started: 11 September 2018

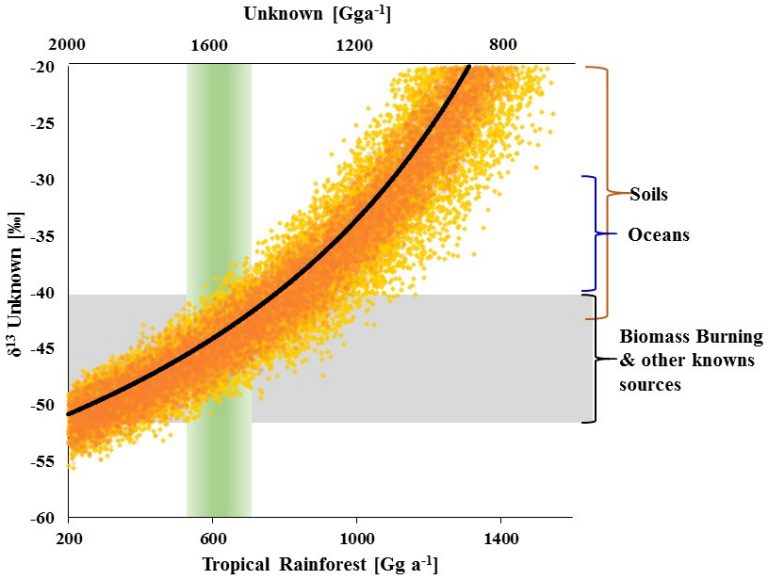

Figure 5: Modeled isotopic composition of the missing source versus tropical rainforest emissions on the lower x-axis and missing emissions on the upper x-axis (rainforest = 2200 – unknown). The black line shows the best estimate derived from the mean isotopic source signatures. Orange dots indicate the range uncertainty from uncertainties in the $\delta^{13}C$ of biomass burning (±7‰), ocean net emissions (±6‰) and other known sources (±6‰). Yellow dots mark the additional uncertainty from the $\delta^{13}C$ of the tropical rainforest source ((±10‰). The green column indicates the carbon density based estimate of the rainforest source and the grey bar indicates the range in $\delta^{13}C$ of biomass burning and the mean from all sources excluding the tropical rainforest.